Computers and Mathematics with Applications 61 (2011) 1968–1974

Contents lists available at ScienceDirect

Computers and Mathematics with Applications

journal homepage: www.elsevier.com/locate/camwa

A new approach to the prediction of passenger flow in a transit system

Shu-Zhi Zhao, Tong-He Ni *, Yang Wang, Xiang-Tao Gao

Transportation and Traffic College, Jilin University, Changchun 130025, China

A R T I C L E I N F O

Keywords:
Bus passenger flow
Non-linear prediction
Chaos recognition
Wavelets

A B S T R A C T

A non-linear model is proposed for predicting the rate of passenger flow in a transit system, and its chaotic characteristic is observed. Using wavelets analysis, the passenger flow data for a whole day are decomposed in a multi-scale way to obtain decomposition sequences. Subsequently, a neural network approach is used to predict the sequences. Finally the passenger flow value can be predicted when the predicted sequences are reconstructed. Results show that the present approach is a feasible method for passenger flow prediction.

1. Introduction

There exist many methods of linear sequence forecasting in the open literature, such as the regression forecasting method [1], the time series prediction method [2], etc. Almost all existing methods infer future trends on the basis of a changing time sequence in the past. Non-linear problems are the focus of research in many fields currently, and the forecasting methods includes the Jenkins forecasting method [3], the Markov forecasting method [4], the Grey forecasting method [5], the multi-objective forecasting method [6], etc. Recently, the neural network and the wavelet network have been applied in the transportation field. Though much progress has been made in non-linear forecasting, there are few studies discussing how to forecast the passenger flow in a transit system because of the regularity and randomness of the passenger flow rate, and traditional forecasting methods always lead to inaccurate results. A new method is, therefore, very much needed.

This paper aims at improving the prediction accuracy for passenger flow forecasting. Firstly, the principal component analysis method is used to observe whether passenger flow data possess chaotic characteristics. Secondly, the passenger flow data are decomposed in a multi-scale way to obtain decomposition sequences which include a smooth and approximate signal and a series of interferences signals with similar frequency and random characteristics on the same scale. Thirdly, a neural network approach is used to obtain predicted sequences with the decomposition sequences as input. Finally, the passenger flow value can be predicted when the predicted sequences are reconstructed. Empirical analysis shows that the proposed model is effective and its precision is preferable.

2. Chaos recognition

2.1. A summary of the chaos recognition method

Chaos [7] is a phenomenon which seems regular and random in a deterministic system. It commonly exists as complex motion and natural phenomena. In addition, it also shows its complexity and randomness in a system. Many different methods of chaos recognition have appeared, such as the power spectrum method [8], the Lyapunov method [9], the Poincaré section method [10] and the principal component analysis method [11]. Comparative studies show that the principal component analysis method can obtain a preferable performance among alternatives. On the basis of fewer data, it can effectively identify chaotic signals by using the principal component spectrum. When the principal component spectrum

* Corresponding author. Tel.: +86 13504439178.
E-mail address: nile1949@yahoo.com.cn (T.-H. Ni).

0898-1221/$ – see front matter
doi:10.1016/j.camwa.2010.08.023

is a straight line with negative slope and it passes through a fixed point, then the signal is chaotic. Hence, the principal component analysis method is easy to observe and analyze.

2.2. The principal component analysis method

The basic steps of the principal component analysis method are summarized as follows [12]:

1. A one-dimensional time series $\{x_1, x_2, \dots, x_n\}$ is given, and its the sampling time interval is τ. Then the phase space is reconstructed with the embedded dimension of d. The trajectory matrix $X_{l\times d}$ $(l = N - (d-1))$ that is formed by the time series is given by

$$X_{l\times d} = \frac{1}{l^{\frac{1}{2}}}\begin{bmatrix} x_1 & x_2 & \dots & x_d \\ x_2 & x_3 & \dots & x_{d+1} \\ \dots & \dots & \dots & \dots \\ x_l & x_{l+1} & \dots & x_N \end{bmatrix}. \tag{1}$$

2. Next, the covariance matrix A is computed as

$$A_{d\times d} = \frac{1}{l}X^T_{l\times d}X_{l\times d}. \tag{2}$$

3. Then, the eigenvalues λ_i $(i = 1, 2, \dots, d)$ and eigenvectors U_i $(i = 1, 2, \dots, d)$ of the covariance matrix A are worked out. The eigenvalues are arranged in descending order: $\lambda_1 \ge \lambda_2 \ge \dots \ge \lambda_d$, the sum of which is computed as

$$\gamma = \sum_{i=1}^{d} \lambda_i. \tag{3}$$

4. Finally, let index i form the X axis, and let $\ln(\lambda_i/\gamma)$ form the Y axis; then the principal component spectrum is obtained. Due to the significant differences between the chaotic signal and the noise signal, the principal component spectrum of the noise is a straight line that is parallel to the X axis. However, the principal component spectrum of the chaotic signal is a straight line through the fixed point with negative slope.

3. Non-linear prediction

The transit passenger flow data are regarded as a signal S with length N. The approximate signal and random interference signals can be obtained when the signal S is decomposed. A neural network approach is used to predict the sequences with the decomposition sequences used for training and testing. The passenger flow value can be predicted when the predicted sequences are reconstructed ultimately.

3.1. Signal decomposition

After decomposition, the signal S produces two sets of parameters. One is the approximate signal cA_1, which is filtered by low-pass filter Lo_D. The other is the detailed signal cD_1, which is obtained from the high-pass filter Hi_D. The two signals are samples with a scale of 2. Then the low-frequency signal cA_1 is regarded as a new signal to re-decompose. This process is continued until a smooth and approximate signal and a series of noise interference signals with similar frequencies have been elicited. Now, $n + 1$ groups of decomposition sequences ($cD_1, cD_2, \dots, cD_n$ and cA_n) are given. Among the decomposition sequences, cA_n characterizes features of signal S, and the cD_n $(n = 1, 2, \dots, n)$ show the subtle fluctuation.

An algorithm provided by the Mallat system aims to decompose and reconstruct signals. Its ideology is: Let there be finite energy signal H_jf which is an approximation of the sum of the approximate signal $H_{j-1}f$ and the interference signal $D_{j-1}f$ with a resolution of 2^{j-1}. Let φ be the scaling function, and let ψ be the wavelet function; thus, the approximate signal $H_{j-1}f$ and interference signal $D_{j-1}f$ are defined as follows:

$$H_{j-1}f(x) = \sum_{k=-\infty}^{+\infty} a_k^{j-1}\varphi(2^{j-1}x - k) \tag{4}$$

$$D_{j-1}f(x) = \sum_{k=-\infty}^{+\infty} d_k^{j-1}\psi(2^{j-1}x - k) \tag{5}$$

where a_k^{j-1} is the roughness coefficient in Eq. (4), and d_k^{j-1} is the detailed coefficient in Eq. (5). Further, the approximate signal of H_jf with a resolution of 2^{j-1} is given by

$$H_jf = H_{j-1}f + D_{j-1}f \tag{6}$$

$$H_jf(x) = \sum_{k=-\infty}^{+\infty} a_k^j\varphi_{j,k}(x). \tag{7}$$

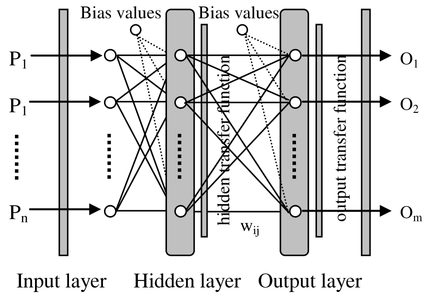

Fig. 1. Structure of the neural network.

For the signal decomposition, let $f \in V_j$; thus, $H_j f = f$. Eq. (6) can equivalently take the following form:

$$f = \sum_{k\in z} \langle f, \varphi_{j-1}, k\rangle \varphi_{j-1,k} + \sum_{k\in z} \langle f, \psi_{j-1}, k\rangle \psi_{j-1,k}. \tag{8}$$

In such a case, the information of space V_j is decomposed into the sub-spaces V_{j-1} and W_{j-1}. Here, $\{\langle f, \varphi_{j-1,k}\rangle\}$ determines the spaces V_{j-1}, while $\{\langle f, \psi_{j-1,k}\rangle\}$ determines the spaces W_{j-1} separately. With such a measure, Eq. (8) is used for computing the inner product and then it can be written as

$$\begin{cases} \langle f, \varphi_{j-1,l}\rangle = \dfrac{\sqrt{2}}{2} \displaystyle\sum_{k\in z} \overline{h_{k-2l}} \langle f, \varphi_{j,k}\rangle \\ \langle f, \psi_{j-1,l}\rangle = \dfrac{\sqrt{2}}{2} \displaystyle\sum_{k\in z} (-1)^k h_{1-k+2l} \langle f, \varphi_{j,k}\rangle. \end{cases} \tag{9}$$

3.2. Neural network simulation and prediction

The neural network is suitable for non-linear prediction [13]. The transit passenger flow data are decomposed into the low-frequency signals cA_n and high-frequency signals cD_n $(n = 1, 2, \ldots, n)$. Due to the advantage that the neural network approach can achieve arbitrary non-linear mapping, it is used to predict the sequences. The model structure has three layers named the input layer, the hidden layer and the output layer, as shown in Fig. 1.

The w_{ij} and T_{ij} are model parameters often called connection weights, and they are revised at the beginning of network learning.

The values of the input nodes are x_i, and the y_i are the values of the hidden layer nodes; then value of the output layer is O_l. The value of the expected output is t_l. The logistic function is often used as a hidden layer transfer function, which is shown as Eq. (10):

$$f(x) = \text{logsig}(x) = \frac{1}{1 + \mathrm{e}^{-x}}. \tag{10}$$

The output nodes of the hidden layer and the output layer have the mathematical representations shown in Eqs. (11) and (12):

$$y_i = f\left(\sum_j w_{ij} x_j - \theta_i\right) = f(\text{net}_i) \tag{11}$$

$$O_l = f\left(\sum_i T_{li} y_i - \theta_l\right) = f(\text{net}_l) \tag{12}$$

where θ is threshold value of each layer. The error function E leads to a decrease in the negative gradient direction, and it can be computed as

$$E = \frac{1}{2} \sum_l (t_l - O_l)^2 = \frac{1}{2} \sum_l (t_l - f(T_{li} f(\text{net}_i) - \theta_l)). \tag{13}$$

The parameters of the neural network are estimated such that the error function is minimized. Thus, the predicted sequences are obtained from the output when the output error is less than 0.01.

3.3. Signal reconstruction

In this section, predicted sequences are reconstructed for recovering the original signal. The approximate signal cA_n and the detailed signal cD_n are reconstructed to obtain cA_{n-1} by low-frequency and high-frequency filtering. This process is continued until the original signal $\hat{s}_i$ emerges.

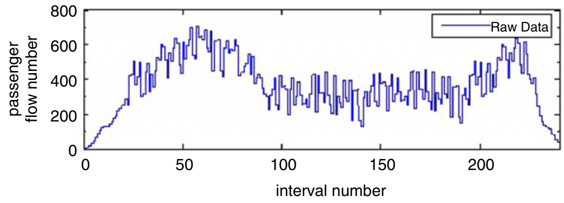

Fig. 2. The passenger flow data for the third bus line on October 19th, 2009.

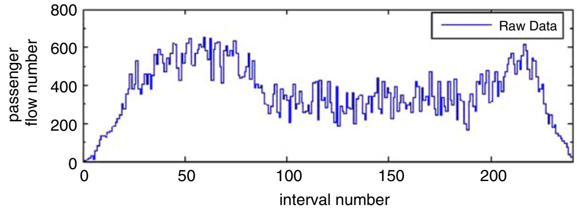

Fig. 3. The passenger flow data for the third bus line on October 20th, 2009.

According to the orthogonality of function $\{\varphi_{j,k}\}$, thus, $f = \varphi_{j,k}$ is extracted from Eq. (9), and it is given by

$$\langle \varphi_{j,k}, \varphi_{j-1,l} \rangle = \frac{\sqrt{2}}{2} \overline{h_{k-2l}} \langle \varphi_{j,k}, \psi_{j-1,l} \rangle = \frac{\sqrt{2}}{2} (-1)^k h_{1-k+2l}. \tag{14}$$

When $f = \varphi_{j,k}(x)$, the inverse form of the scale equation can be written as

$$\varphi_{j,k}(x) = \sum_{l \in z} \frac{\sqrt{2}}{2} \overline{h_{k-2l}} \varphi_{j-1,l}(x) + \sum_{l \in z} \frac{\sqrt{2}}{2} (-1)^k h_{1-k+2l} \psi_{j-1,l}(x). \tag{15}$$

By computing the inner product of Eq. (15), the reconstruction formula is obtained, as shown in Eq. (16):

$$\langle f, \varphi_{j,k} \rangle = \sum_{l \in z} \frac{\sqrt{2}}{2} h_{k-2l} \langle f, \varphi_{j-1,l} \rangle + \sum_{l \in z} \frac{\sqrt{2}}{2} (-1)^k \overline{h_{1-k+2l}} \langle f, \psi_{j-1,l} \rangle. \tag{16}$$

The reconstructed signal s is the prediction for data for the bus passenger flow in the next period.

3.4. Error testing

In this section, the average absolute error and mean square error are adopted to represent differences between the actual value and the predicted value.

Let there be an actual value s_i, and let $\hat{s}_i$ be the predicted value; thus, the average absolute error is given by

$$AAE = \frac{1}{N} \sum_{i=1}^{n} \left| s_i - \hat{s}_i \right|. \tag{17}$$

Further, the mean square error is written as

$$MSE = \frac{1}{N} \sqrt{\sum_{i=1}^{n} (s_i - \hat{s}_i)^2}. \tag{18}$$

4. Empirical analysis

This study investigates the third bus line in Liaoyuan City, Jilin Province. The whole length of the line is 13.5 km, and line is equipped with 21 standard buses each of which can take 19 passengers. The average interval in the peak period and off-peak hours is 3 min. From the railway station to the terminal named 'Five-star', 240 runs depart every day. Taking 3 min as the interval, this study recorded the passenger flow data for October 19th, 2009, as shown in Figs. 2 and 3.

Using the principal component analysis method, the principal component spectra are as shown in Figs. 4 and 5.

The results from these figures show that the passenger flow data are in accordance with the chaos characteristic.

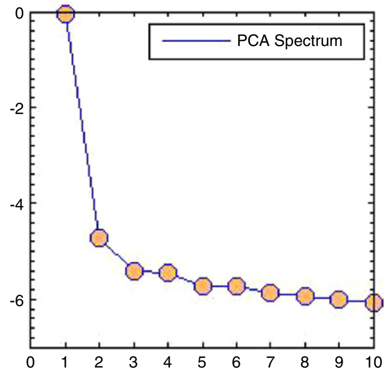

Fig. 4. The principal component spectrum on October 19th.

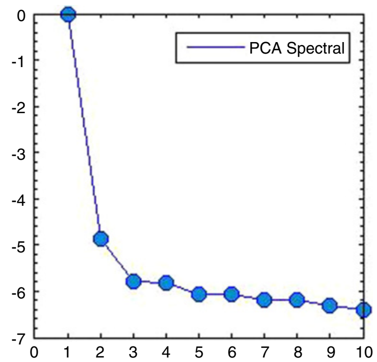

Fig. 5. The principal component spectrum on October 20th.

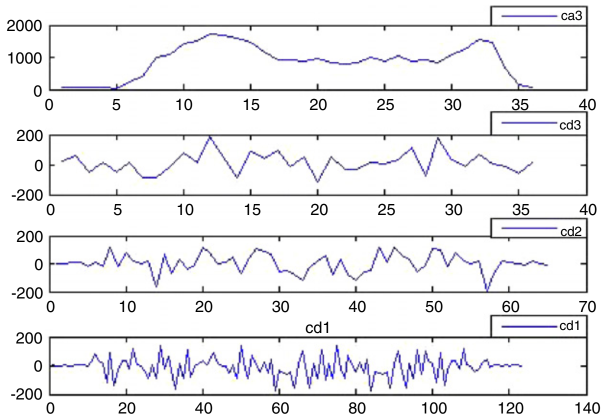

Fig. 6. The decomposition sequences of the data for October 19th.

Further, the passenger flow data for October 19th and 20th are decomposed using the wavelet function db4; then, the low-frequency signal cA_3 and the high-frequency signals cD_n $(n = 1, 2, 3)$ are obtained, as shown in Figs. 6 and 7.

The neural network approach is used to predict the sequences, with the first half of cA_3 and cD_n $(n = 1, 2, 3)$ as input. The training and testing is continued until the error is below 0.01. Then, the predicted sequences are obtained, as shown in Fig. 8.

The low-frequency section and the high-frequency section of the predicted sequences are reconstructed using the db4 wavelet function. Finally, the passenger flow value on October 21th can be predicted. Fig. 9 shows the comparison between the predicted data and actual data.

The absolute error and the mean square error are computed as shown in Figs. 10 and 11.

The result of the comparison between the predicted data and actual data indicates that the proposed model has been shown to be effective, and the error is acceptable.

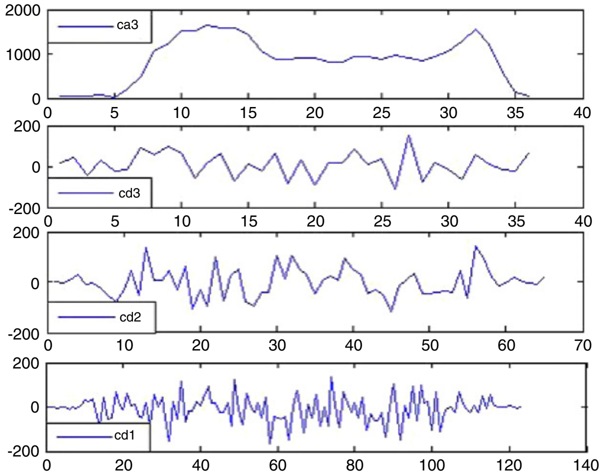

Fig. 7. The decomposition sequences of the data for October 20th.

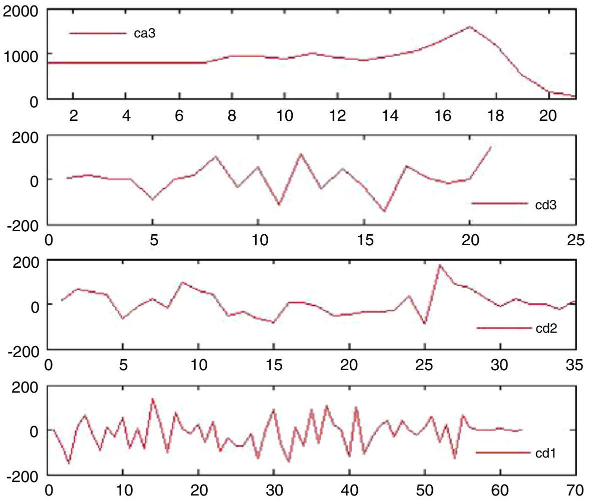

Fig. 8. The predicted sequences.

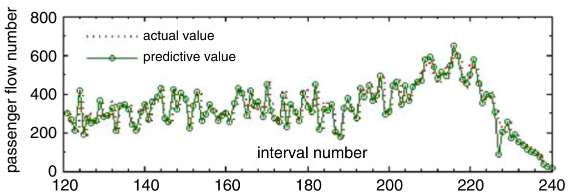

Fig. 9. The comparison between the predicted data and actual data for October 21th.

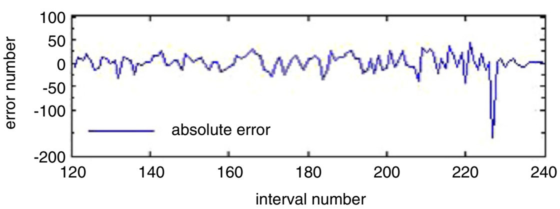

Fig. 10. The absolute error.

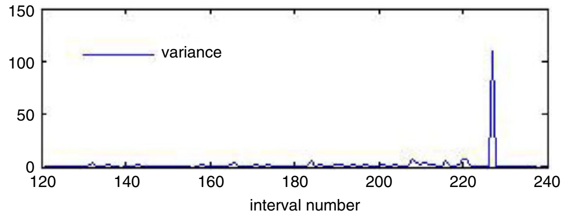

Fig. 11. The mean square error.

5. Conclusion

In this study, wavelet analysis and a neural network are applied to propose a non-linear model for predicting the rate of passenger flow. The study concludes that transit passenger flow data have chaos characteristics. This promising result illustrates that the non-linear model presented here is effective with minimal prediction error. Moreover, the model reflects the changes of the passenger flow objectively. Empirical results indicate that the proposed model can provide an effective way to improve predictive performance. Therefore, it could provide a new approach for the prediction of passenger flow and a theoretical basis for bus special planning.

References

[1] K. Nikolopoulos, P. Goodwin, A. Patelis, V. Assimakopoulos, Forecasting with cue information: a comparison of multiple regression with alternative forecasting approaches, European Journal of Operational Research 180 (2007) 354–368.
[2] T. Miyano, S. Kimoto, H. Shibuta, K. Nakashima, Y. Ikenaga, K. Aihara, Time series analysis and prediction on complex dynamical behavior observed in a blast furnace, Physica D 135 (2000) 305–330.
[3] Y. Lu, S.M. AbouRizk, Automated Box–Jenkins forecasting modeling, Automation in Construction 18 (2009) 547–558.
[4] Md. Rafiul Hassan, A combination of hidden Markov model and fuzzy model for stock market forecasting, Neurocomputing 72 (2009) 3439–3446.
[5] Chin-Tsai Lin, Shih-Yu Yang, Forecast of the output value of Taiwan's opto-electronics industry using the Grey forecasting model, Technological Forecasting and Social Change 70 (2003) 177–186.
[6] Pao-Shan Yu, Shien-Tsung Chen, Chia-Jung Chen, Tao-Chang Yang, The potential of fuzzy multi-objective model for rainfall forecasting from typhoons, Natural Hazards 34 (2005) 131–150.
[7] Upadhyay S.H., Jain S.C., Harsha S.P., Chaos and nonlinear dynamic analysis of high-speed rolling element bearings due to varying number of rolling elements, International Journal of Nonlinear Sciences and Numerical Simulation 10 (2009) 323–332.
[8] Zsolt Bozóki, Chaos theory and power spectrum analysis in computerized cardiotocography, European Journal of Obstetrics & Gynecology and Reproductive Biology 71 (1997) 163–168.
[9] Hongbin Zhang, Chunguang Li, Jian Zhang, Xiaofeng Liao, Juebang Yu, Controlling chaotic Chua's circuit based on piecewise quadratic Lyapunov functions method, Chaos, Solitons & Fractals 22 (2004) 1053–1061.
[10] Jang-Der Jeng, Yuan Kang, Yeon-Pun Chang, An alternative Poincaré section for high-order harmonic and chaotic responses of a rubbing rotor, Journal of Sound and Vibration 328 (2009) 191–202.
[11] Lin-nan Yang, Lin Peng, Li-min Zhang, Li-lian Zhang, Shi-sheng Yang, A prediction model for population occurrence of paddy stem borer (Scirpophaga incertulas), based on back propagation artificial neural network and principal components analysis, Computers and Electronics in Agriculture 68 (2009) 200–206.
[12] Nils Lehmann, Principal components selection given extensively many variables, Statistics & Probability Letters 74 (2005) 51–58.
[13] T. Kerh, G.S. Hsu, D. Gunaratnam, Forecasting of nonlinear shoreline variation based on aerial survey map by neural network approach, International Journal of Nonlinear Sciences and Numerical Simulation 10 (2009) 1211–1221.